Could road constructions be more disastrous than an earthquake in terms of landsliding?

Hakan Tanyaş[1,2], Tolga Görüm[3], Dalia Kirschbaum[1], Luigi Lombardo[4]

[1]NASA Goddard Space Flight Center, Hydrological Sciences Laboratory, Greenbelt, MD, USA

[2]USRA, Universities Space Research Association, Columbia, MD, USA

[3] Istanbul Technical University, Eurasia Institute of Earth Sciences, Istanbul, Turkey

[4]University of Twente, Faculty of Geo-Information Science and Earth Observation (ITC), Enschede, Netherlands

Corresponding author: Hakan Tanyaş (hakan.tanyas@nasa.gov)

Key Points:

- We report a distinct correlation of mass movements and major road constructions
- Poor engineering practices threat not only local communities but also biodiversity
- The impact of road construction can disturb the natural slope equilibrium to an extent comparable with moderate (> 6 M_w) earthquakes

Abstract

Roads can have a significant impact on the frequency of mass wasting events in mountainous areas. However, characterizing the extent and pervasiveness of landslides over time rarely been documented due to limitations in available data sources to consistently map such events. We monitored the evolution of a road network and assessed its effect on slope stability for a ten year window in Arhavi, Turkey. The main road construction projects run in the area are associated with a hydroelectric power plant as well as other road extension works and are clearly associated with the vast majority (90.1%) of mass movements in the area. We also notice that the overall number and size of the landslides are much larger than in the naturally-occurring comparison area. This marks a strong and negative effect of human activities on the natural course of earth surface processes. Our findings show that the damage generated by the road construction is compatible with the possible effect of a theoretical earthquake with a magnitude greater than M_w=6.0. Overall, better co- and post-construction conditions should be ensured during and after road works to mitigate the risk to local communities. We also notice a significant variation in sediment transport as a result of road construction. As a result, our study fits in the big picture of Anthropocene related changes and specifically points out at problems in mountainous areas that could undoubtedly be better managed to reduce the risk to local communities.

1 Introduction

Recent findings suggest that our planet has been going through a new geologic time, Anthropocene, in which human-driven changes dominate the Earth system and its geological records instead of natural processes (e.g., Lewis & Maslin, 2015; Steffen, Broadgate, Deutsch, Gaffney, & Ludwig, 2015). The existence of the Anthropocene is supported by the "*Great Acceleration*" graphs showing proxies of growing human activities (e.g., population, water use, transportation, etc.,) and their influence on natural systems (e.g., CO2 emission, surface temperature, domesticated land, etc.,), which becomes quite obvious since the mid-20th century (Steffen et al., 2015; Steffen, Grinevald, Crutzen, & McNeill, 2011) and is functionally and stratigraphically distinct from the Holocene epoch (Waters et al., 2016). However, the existence of the Anthropocene still needs much evidence (Brown et al., 2013). Notably, soil erosion, as a geomorphologic process, has an essential role in the formation of the geological record. In fact, soil erosion in the Anthropocene is chiefly governed by the coupled effect of natural and human-

induced soil erosion processes (Poesen, 2018). In this context, we still need to better understand the interactions between these processes (Brown et al., 2017).

In seismically active mountain ranges, landslides appear as the major erosive agent (e.g., Dadson et al., 2004; Morin et al., 2018; Parker et al., 2011). Moreover, anthropogenic factors (i.e., land-use change, deforestation, hill cutting, etc.,) can also be a significant contributor of landslide initiations in active mountain ranges (e.g., Chang & Slaymaker, 2002; Holcombe, Beesley, Vardanega, & Sorbie, 2016; Larsen & Parks, 1997; Vuillez et al., 2018). In particular, road construction is reported as one of the most influential factors of landslide occurrence in seismically active mountainous regions such as in India (e.g., Barnard, Owen, Sharma, & Finkel, 2001; Haigh, Rawat, & Bartarya, 1989), Nepal (e.g., Hearn & Shakya, 2017; McAdoo et al., 2018), New Zealand (e.g., Coker & Fahey, 1993; Fransen, Phillips, & Fahey, 2001), Pakistan (e.g., Atta-ur-Rahman, Khan, Collins, & Qazi, 2011; Owen et al., 2008) and Taiwan (e.g., Chang & Slaymaker, 2002; Chen & Chang, 2011). This is not a surprising because hillslope cutting can cause a reduction in shear strength of hill slope material and also raised or perched water tables that lead to increase pore water pressure in case of rainfall event (Holcombe et al., 2016).

As a result, we observe an increasing number of slope failures in seismically active mountain ranges such as the Himalayan region because of road construction (e.g., Froude & Petley, 2018; D. N. Petley et al., 2007). However, capturing the anthropogenic effect in landslide occurrence may not be a trivial task in such environments because seismicity disturbs rock masses and increases landslide susceptibility irrespective of road construction (e.g., Owen et al., 2008; Tang, Zhu, Qi, & Ding, 2011). Therefore, differentiating the signal of anthropogenic effect from the seismic one can be a challenge in some cases. For instance, Khattak et al. (2010) and Khan et al. (2013) examine the post-seismic landslide evolution following the 2015 Kashmir earthquake and emphasize the possible confusion between landslides triggered by road construction and strength reduction caused by seismic shaking. The same difficulty distinguishing the contribution of anthropogenic and seismic factors in landslide occurrence can also be valid for slope failures that occurred following the 2015 Gorkha earthquake. Jones et al. (2020) report an increased landslide rate from 2016 to 2018, which is argued to be primarily associated with the increase in road-construction efforts. However, the disturbance induced by the earthquake is inevitably a part of the predisposing factors.

This implies that capturing the anthropogenic effect could be more convenient in an environment at which seismicity does not play a significant role in landslide occurrence. Therefore, in this study, we focus on a mountainous area located in the northeastern part of Turkey, where the site has been exposed to no significant seismicity but to multiple road construction projects. We examine not only expanding roads, but also mass movements associated with those roads over the last 10 years. To assess the role of the anthropogenic effect, we also map landslides that do not show any direct relation with roads. Ultimately, we compare our landslide inventory triggered by hillslope cutting and a landslide inventory associated with an earthquake, which is one of the most common triggers (D. Petley, 2012). By this comparison, we aim to better assess how relevant human influence can be compared to natural processes.

2 Study area

The study area is located in the northeastern part of Turkey within the municipal boundaries of Fındıklı, Rize, and Arhavi, Artvin. It comprises nine catchments over approximately 195 km^2 (Fig. 1). Volcanics and volcaniclastics are the main geological units seen in the study area (MTA, 2002). Specifically, the alternation of basalt-andesitic lava, pyroclastics, sandstone, marl, and clayey limestone has been observed throughout the area (Alan et al., 2019).

The study area extends approximately 25 km from the coastline and within the zone, elevation sharply increases to 3350 m from the sea level. This reflects the steep topography in the area. The maximum slope steepness within the examined area is 72º, whereas the average slope steepness is 29º±11º.

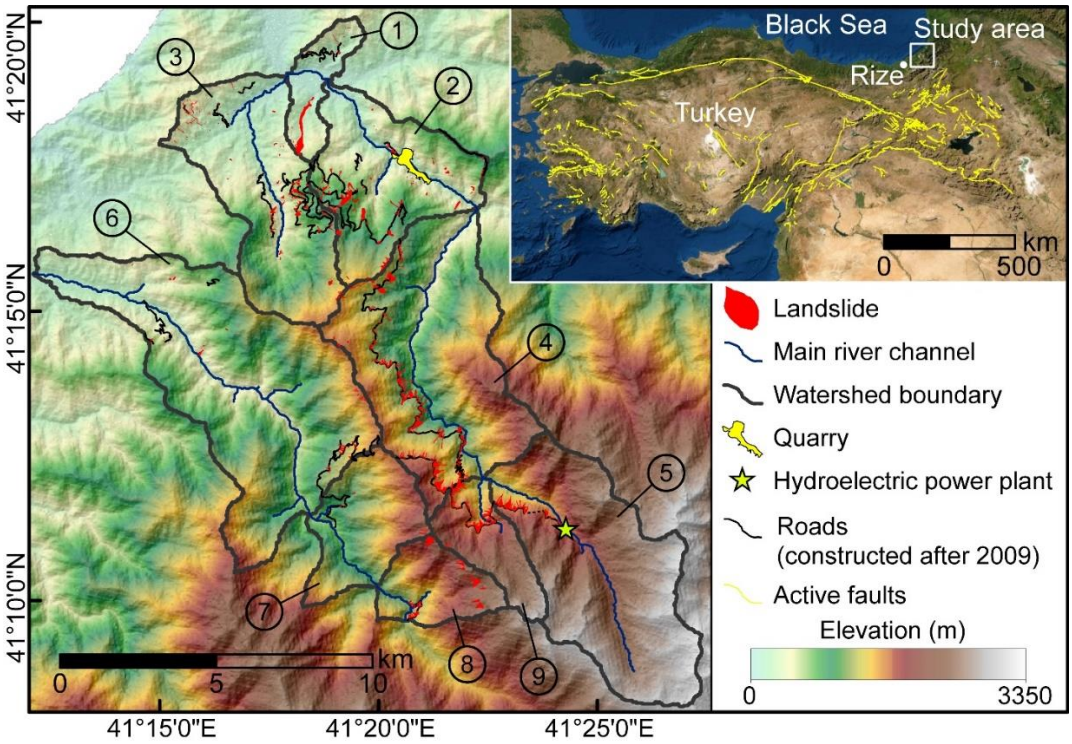

Figure 1. Overview of the study area. Catchments are labelled by numbers.

The steep topographic features of the site are coupled with a strong precipitation regime. The study area is within the zone receiving the highest precipitation measured throughout Turkey (Fig. 2a). Based on the 20 years (from 2000-06-01 to 2020-03-31) time series of the Integrated Multi-Satellite Retrievals (IMERG) Final Run product (Huffman, Stocker, T, Nelkin, & Tan, 2019), which is available through Giovanni (v.4.32) (Acker and Leptoukh, 2007) online data system, the average monthly precipitation of extreme events (i.e., above 0.95 quantile) is 353±40 mm/month. The same dataset also shows that the average daily precipitation of extreme events is 39±17 mm/day.

As for the seismicity, the study area has not been exposed to strong external forces caused by earthquakes. It is approximately 270 km from the North Anatolian Fault Zone (Fig. 1). The Earthquake catalog of U.S. Geological Survey (2017) shows that in the last 100 years no earthquake (M_w>3) occurred within a buffer zone of 50 km radius centered within the study area (Fig. 2b). The largest earthquake (M_w=6.8) occurred in 1983, approximately 120 km southeast of the study area. Except for this event, only seven earthquakes of magnitude larger than 5.0 have occurred in the near vicinity and the closest epicentral location is 70 km away from the study area.

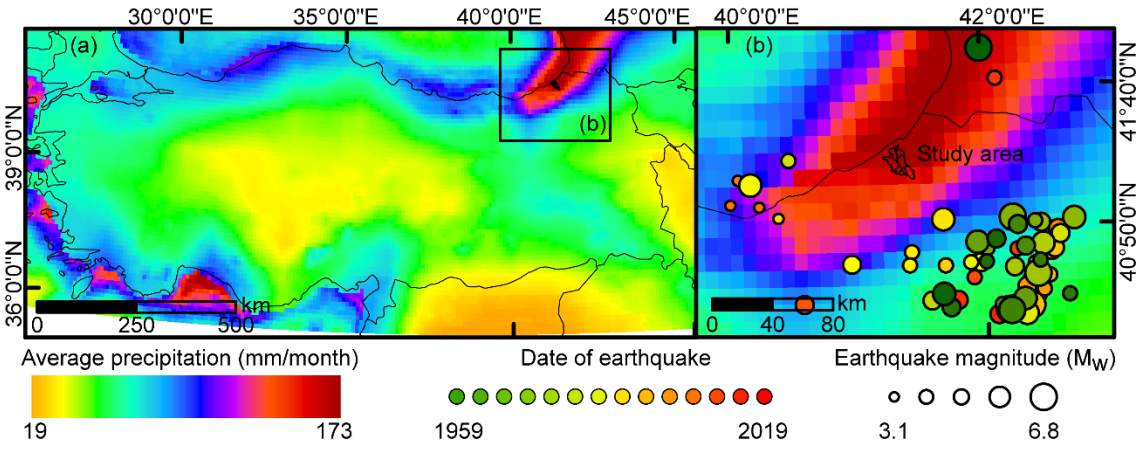

Figure 2. Maps showing the characteristics of the study area regarding (a) the precipitation amounts that is the highest of entire Turkey (Huffman et al., 2019) and (b) the seismic record of the area for earthquakes occurred after 1900 (U.S. Geological Survey, 2017).

Although the site has not been exposed to strong seismicity, landslides are one of the main natural hazards threatening the East Black Sea region and extreme precipitation, land-use change and road construction are the most common factors causing landslides (e.g., Nefeslioglu, Gokceoglu, Sonmez, & Gorum, 2011; Raja, Çiçek, Türkoğlu, Aydin, & Kawasaki, 2017; Reis, Nişanci, & Yomralioğlu, 2009). During the last decade, an increasing number of road construction projects has been increasing the landslide susceptibility in the Black Sea Region (e.g., Raja et al., 2017). In particular, within our study area, road constructions have a significant role in landslide occurrences (Akbulut & Kurdoglu, 2015). Road construction has been conducted for three main reasons: (1) to increase the accessibility to highlands to boost tourism in the region (*Green Road project*, DOKAP, 2014), (2) to build a hydroelectric power plant (HEPP) in the southern part of the study area and (3) to improve the road network overall. Some of the roads constructed under the third category could be indirectly associated with the first two classes because newly constructed roads may have further stimulated the construction of others.

These construction projects are met with resistance from both non-governmental environmental organizations (e.g., WWF, 2020) and geoscientific community (e.g., Akbulut & Kurdoglu, 2015) because the study area is within the Caucasus ecoregion, which is one of the world's 34 biodiversity hotspots (Şekercioğlu, Anderson, Akçay, Bilgin, et al., 2011). The Kamilet Valley crossing through the study area (Sub-basins 4, 5 and 9 in Fig. 1) is one of the sites reflecting the rich biodiversity of the region. It hosts numbers of endemic and rare non-endemic plants species that need to be protected (Akbulut & Kurdoglu, 2015; Şekercioğlu, Anderson, Akçay, & Bilgin,

2011; Yuksel & Eminagaoglu, 2017). Therefore, the research question of this study -- that aims at exploring the anthropogenic control on hillslope erosion processes -- also has implications on the protection and sustainable development of a biodiversity hot spot.

3 Materials and method

We map both landslides and constructed roads from 2010 to June 2020. To create these multi-temporal inventories, we use PlanetScope (3-5 m), Rapid Eye (5 m) images acquired from Planet Labs (Planet Team, 2017) and high-resolution Google Earth scenes. The details of the satellite images we used are presented in Table S1.

We create inventories based on the systematic examination of satellite images through manual mapping. We always compare two images to map landslides that occurred and roads that were constructed within the examined time window. We do not follow a fixed temporal resolution to map landslides or roads. In fact, we aim at using all the available cloud-free satellite images. Thus, the resulting temporal resolution of the landslide inventories is not fixed and actually increases after 2016, following the increase in the number of available images. For instance, the temporal resolution of our inventory is approximately one year between 2010 and 2011, whereas, after 2016, it is much finer at up to one-month frequency (Table S1).

While mapping, we examine whether or not landslides are associated with road construction. For this binary labelling, we manually go through the inventory and identify the ones having contact with roads. If the target landslide crosses a road or is initiate right under a road cut, we label the given landslide as a human-induced one.

Also, we group landslides that occurred and roads that were constructed based on two different criteria, namely, by assigning a label describing the purpose of road construction and the occurrence/construction time. For the former one, we examine the purpose of road constructions and categorize them under three headings: (1) HEPP project, (2) Green Road project and (3) others (i.e., roads constructed after 2010 for other reasons than Green road and HEPP projects). Using the same classification, we label not only roads but also the corresponding landslides. We also compare landslides associated with road constructions and the ones triggered by precipitation. We do so by examining the occurrences of landslides for different catchments.

This allows us to better investigate the anthropogenic influence by comparing two adjacent catchments exposed to different levels of external disturbances caused by road construction.

For the second criterion, we label landslides/roads using one year of fixed temporal windows. As a result, we create 11 temporal categories that we can use to examine the evolution of both landslides and roads from 2010 to June 2020 with one year temporal resolution. We do not differentiate source and depositional areas of landslides and delineate them as a part of the same polygon. If the existing landslides expand over time, we only map the new surface in the examined time window.

To examine the landscape characteristics and precipitation regimes, we use Shuttle Radar Topography Mission (SRTM) digital elevation models (approximately 30-m resolution) (NASA JPL, 2013) and the Global Precipitation Measurement (GPM), the Integrated Multi-Satellite Retrievals (IMERG) Final Run product (Huffman et al., 2019).

Ultimately, we compare our human-induced mass movement inventory with a sample of earthquake-induced landslide inventories, available via the U.S. Geological Survey ScienceBase platform (Schmitt et al., 2017; Tanyaş et al., 2017). We make this comparison to assess how hazardous road construction could be compared to naturally occurring landslides. For the comparison, we examine the landslides' size statistics, which has been used as a basis to identify landslide-event magnitude scale (mLS) and provides a measure to quantify the severity of landslide events (Malamud, Turcotte, Guzzetti, & Reichenbach, 2004). We calculate mLS using the code provided by Tanyaş et al. (2018). We also calculate the slope of the power-law distribution (β, power-law exponent) that the frequency-density distribution of landslides exhibits (e.g., Guzzetti, Malamud, Turcotte, & Reichenbach, 2002; Malamud et al., 2004; Tanyaş, van Westen, Allstadt, & Jibson, 2019) using the method proposed by Clauset et al. (2009). To estimate an earthquake magnitude for an equivalent earthquake-induced landslide inventory with our human-induced one, we use the empirical relation between earthquake magnitude (M) and landslide-event magnitude scale (Malamud et al., 2004).

$$mLS=1.29\times M-5.65 \quad (1)$$

4 Results

4.1 Mapping of roads and landslides

We identified the roads associated with "*HEPP*" and "*Green Road*" projects (Fig. 3a) based on information from our local contacts and interviewees. They informed us about other expansion work conducted along the route of the Green Road project. We could not identify the time of these expansions, but we know the sections where the engineering work was carried out. We labelled the roads that already exist as of January 2010 as "*Pre-2010*" based on our analyses of satellite scenes. We labelled the rest of the roads constructed after 2010 as "*Others*". Based on the identified roads, we also labelled corresponding mass movements (Fig. 3b).

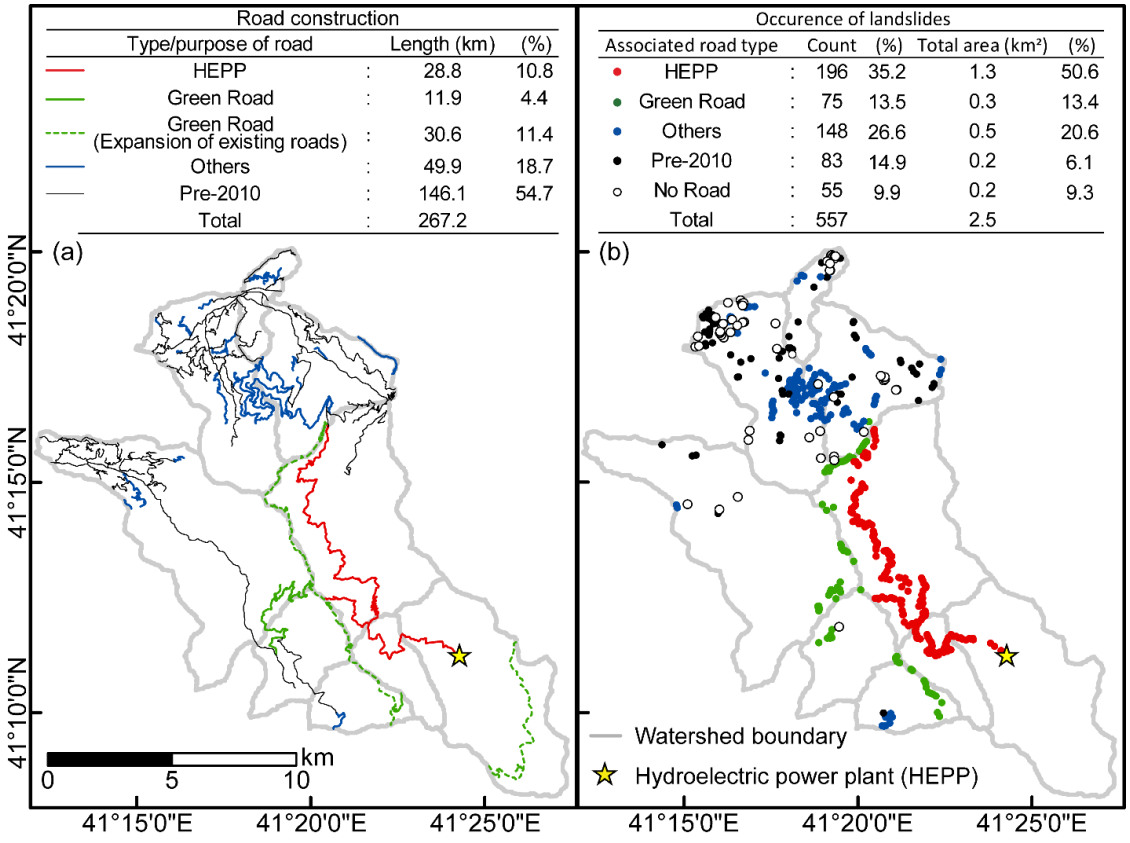

Figure 3. Maps showing the distribution of (a) the roads constructed for different purposes and (b) the associated landslides.

To create these road and landslide inventories, first, we mapped both roads and landslides associated with *HEPP* (Fig. 3). Mapping landslides was particularly challenging because of the short-term interactions between mass movements and engineering activities. Specifically, local people indicated that the excavated hillslope materials were mostly dumped into the river channels during the construction, and also down the slope of the road cut. This may have also induced some landslides further down the hillslope because of the additional load. Notably, this

makes the identification of landslides difficult because the dumped hillslope materials and landslides triggered by the construction are mostly mixed and have a similar appearance in satellite scenes. For instance, Figure 4 shows a segment of the road excavation conducted as part of the *HEPP* project. This satellite image clearly shows that dumped materials are mixed with landslides triggered by road construction. We can both see mass movements that were initiated from the upper or lower hillslopes. For the former ones, we can be sure that these are human-induced landslides. However, for the latter cases, we cannot differentiate whether they are solely dumped materials or human-induced landslides. In fact, most likely, their genesis is the result of the coupled effect of both processes.

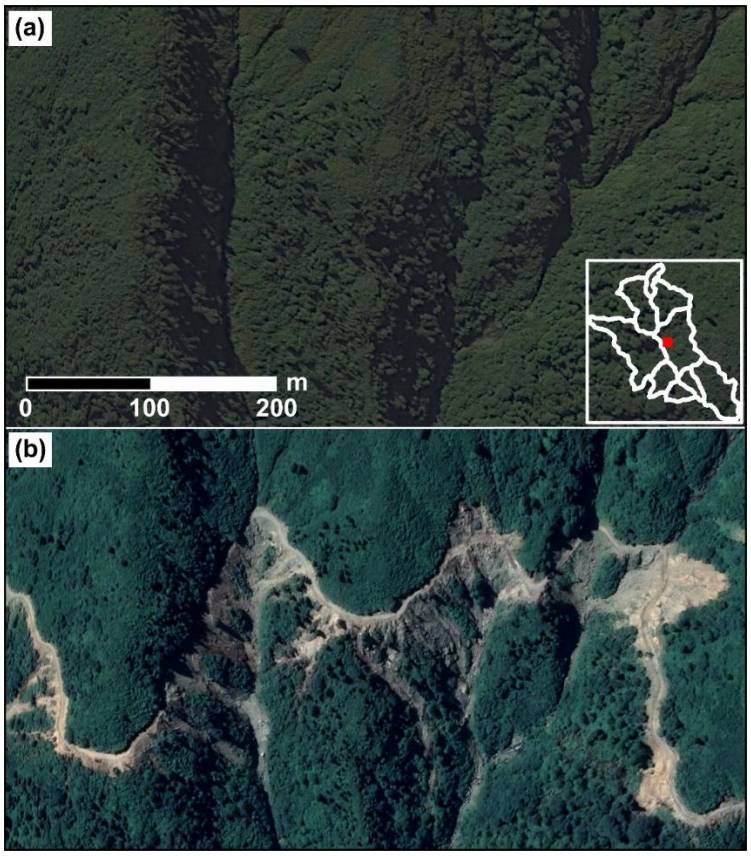

Figure 4. Satellite scenes showing the pre- and post- excavation landscape in a selected area (41º 13′ 56″ N and 41º 20′ 18″ E) along the route excavated for the *HEPP* project. The examined segment of the road was constructed between 17th July 2016 – 6th September 2016. Within the same period, mass movements widely occurred. We also identified some landslides enlarged between 6th September 2016 – 9th July 2017. The location of the sample area is geographically shown in the lower right of the panel (a).

Local interviews also emphasized that the road construction carried out for the *HEPP* project has dramatically affected the natural course of erosional processes since 2016 (Fig. 5). They argue that explosives were used in some parts of the road construction to facilitate the progress of the project. This most likely weakened the shear strength of hillslope material, increasing the landslide susceptibility of the given site and promoting the failures we noted.

Figure 5. Photos showing the mass movements on hillslopes associated with road constructions of *HEPP*. The photos were taken on 15th June 2020 (Photographs courtesy of Hasan Sıtkı Özkazanç).

Overall, the differentiation between dumped materials and human-induced landslides is challenging. Regardless, these processes initiate additional anthropogenic sediment loads to river channels. The local environmental organizations (*Arhavi Doğa Koruma Platformu*) provided evidence to this claim in an early 2020 report where an increased sediment content was noted in the Kamilet River (Fig. 6). Therefore, in this study, we did not differentiate the dumped hillslope materials and landslides; instead, we considered them all as human-induced mass movements.

Figure 6. Photos showing the intersection of Kamilet and Durguna Rivers (41º 16′ 34″ N and 41º 22′ 32″ E) where increased sediment content in Kamilet River caused by the *HEPP* construction is evident. The pictures were taken in May 2020. Location of this spot is given in the lower right of the panel (b) (Photos by Hasan Sıtkı Özkazanç).

We also mapped mass movements that occurred along with the Green Road project (Fig. 3). Some of the mass movements occurred along existing roads, which were expanded in relation to the Green Road project. Similar to the *HEPP* case, dumped hillslope materials might also play a role in these mass movements. However, Figure 7 shows that the crests of some mass movements extend backward from the road and therefore, we argue that these must be a mixture of both dumped materials and human-induced mass movements if they are not purely human-induced mass movements.

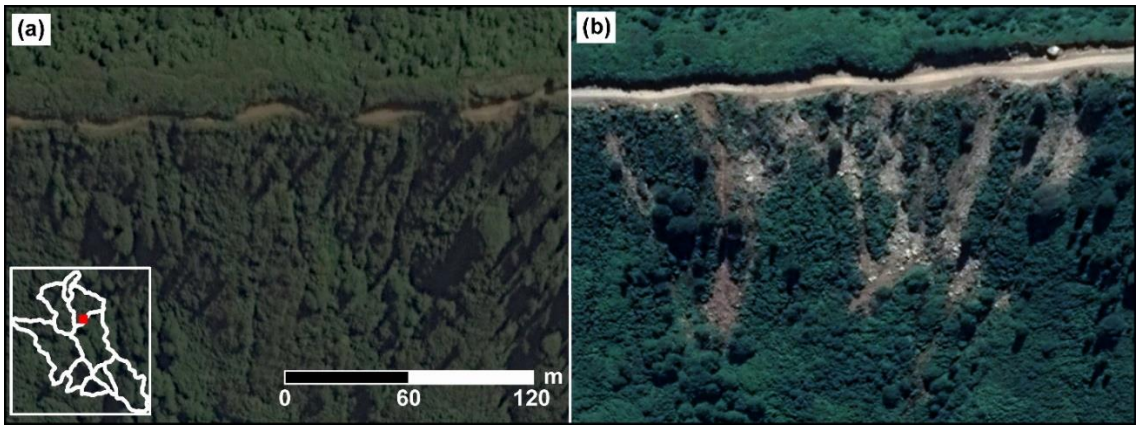

Figure 7. Google Earth scenes showing the pre- and post- expansion landscape at a selected site (41º 15′ 37″ N and 41º 20′ 24″ E) along the route excavated for the Green Road project. Mass movements occurred between 18th September 2017 – 27th May 2018. The location of these mass movements is given in the lower left of panel (a).

Moreover, we mapped mass movements that occurred along other roads (i.e., *Others*) that were excavated during the same period (Fig. 3). These are mostly secondary and private roads opened to access agricultural sites or houses and therefore, they were created without the use of explosive. Consequently, excavated materials are expected to be less compared to HEPP and Green Road, which were designed for higher traffic loads that require a wider road section and cut. Figure 8 shows an example of human-induced mass movements along roads labelled as *Others*.

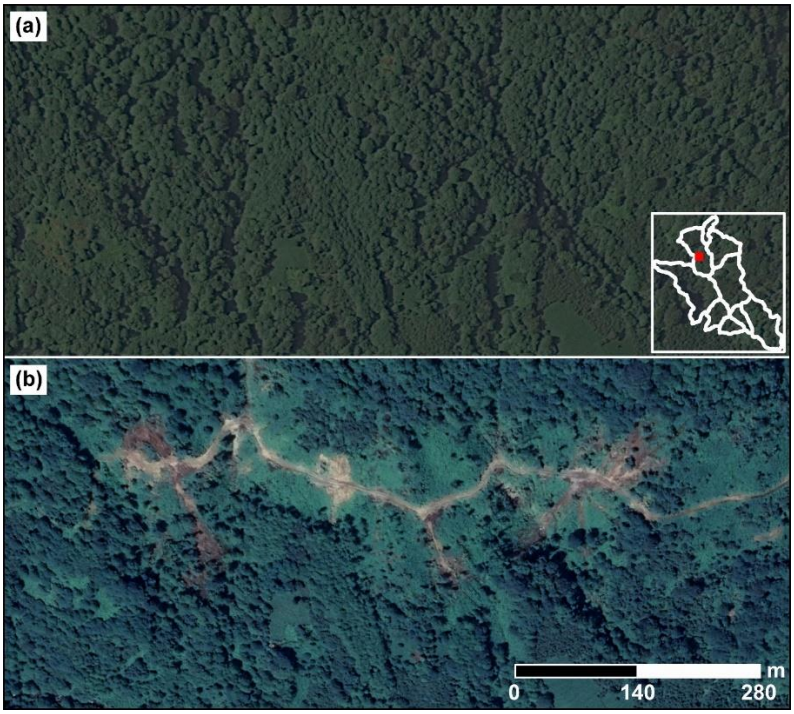

Figure 8. Google Earth scenes showing the pre- and post- road expansion conditions at a selected site (41º 16′ 24″ N and 41º 17′ 51″ E) representing the mass movements categorized as *Others*. The examined the segment of the road constructed between 10th September 2013 – 3rd September 2014. Landslides occurred between 18th November 2017 – 27th May 2018 and 20th March 2019 – 21st May 2019. The location of these mass movements is given at the lower right of the panel (a).

Ultimately, we mapped landslides that occurred along the existing roads (*Pre-2010*) (Fig. 9) and the ones triggered by natural agents irrespective of roads (*No Road*) (Fig. 10). Precipitation is the most likely triggering factor for these landslides. However, for the Pre-2010 case, road works should have played a crucial role in the failure mechanism by disturbing both resisting forces

against sliding and hydrological conditions. As for the *No Road case*, in addition to precipitation as a triggering factor, some anthropogenic factors might have played a role, albeit to a much lesser extent. We will elaborate on the possible contribution of those indirect anthropogenic factors in Section 5.

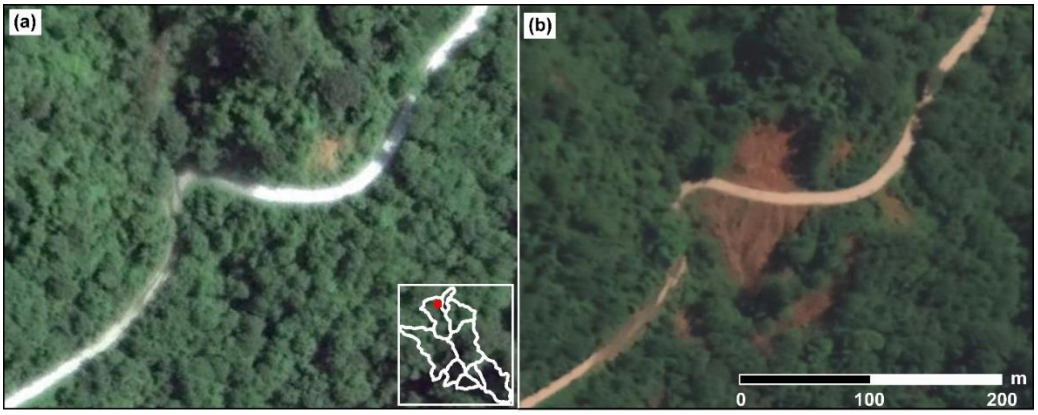

Figure 9. Google Earth scenes showing the pre- and post- landslide views at a selected site (41º 18′ 20″ N and 41º 20′ 14″ E), representing the mass movements that occurred along an existing road (i.e., *Pre-2010*). Mass movements occurred between 3rd November 2016 – 16th April 2017. The location of these mass movements is given in the lower right of the panel (a).

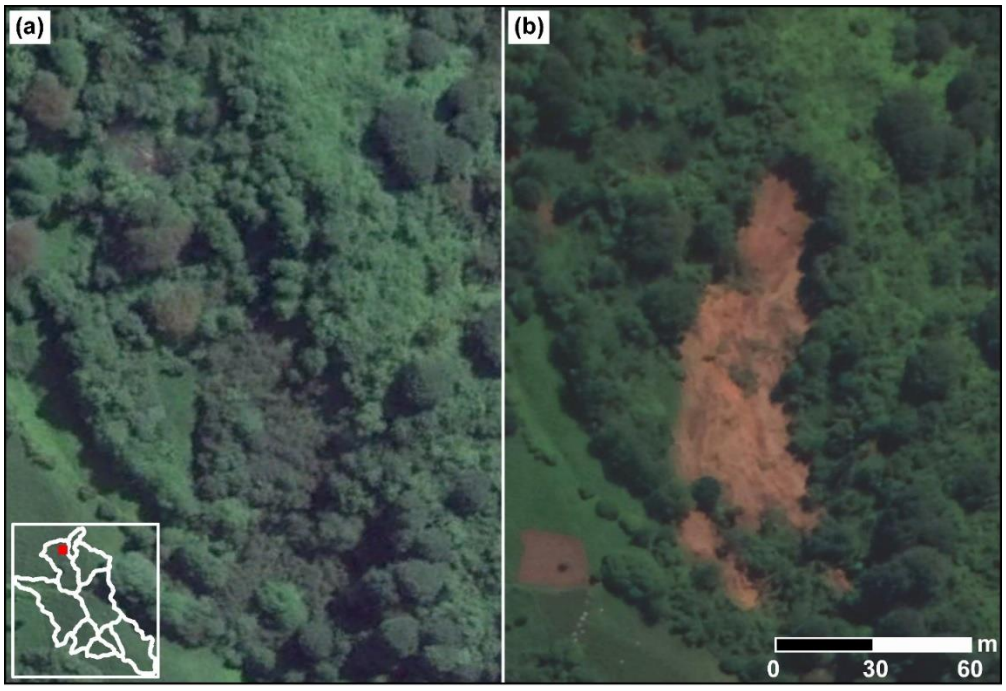

Figure 10. Google Earth scenes showing the pre- and post- landslide landscape at a selected site (41º 18′ 20″ N and 41º 17′ 58″ E) representing the mass movements triggered by natural agents

(i.e., *No Road*). The landslide occurred between 17th July 2016 – 9th September 2016. The location of the landslide is given in the lower left of the panel (a).

4.2 Analyses of mass movements

We mapped 557 mass movements and a 267.2 km long road network. Overall, 33.9% of the roads were developed during the last 10 years, for various purposes (see Fig. 3a). Among them, 10.8% is associated with the *HEPP* project and 4.4% is related to the *Green Road* project. Also, some of the existing roads have been extended in relation to the Green Road project and this contribution refers to 11.4% of all roads in the study area. Moreover, 18.7% of the roads constructed after 2010 are not directly associated with the *HEPP* nor the *Green Road* projects, but some indirect connections could exist (*Others*).

We also examined mass movements in relation to road work. Our findings show that 90.1% of them occurred after 2010 while being in immediate proximity to the roads (Fig. 3b). As for the cumulative area of mass movements, the anthropogenic influence is also significant: 90.7% of total size is associated with road constructions. Roads constructed as part of the *HEPP* project has the most substantial contribution to mass movements occurrences. In the study area, 1.3 km^2 of mass movements were solely caused by the *HEPP* project, which refers to 50.6% of the total size identified in the study area. During the last 10 years, 9.9% of landslide occurred with no direct relationship with roads. In terms of total size, the influence of these landslides constitutes 9.3% of the total area of mass movements. This static summary is complemented below by examining the variation in both road construction and landslide occurrence on a temporal basis (Fig. 11 and 12). We noticed a peak value in road construction in 2012. However, the peak in the constructions does not correspond to a significant number of landslides. This is mainly because of the morphologic conditions encountered through the route. In fact, most of the roads we mapped between 2011 and 2012 are associated with roads categorized as *Others*. The mean slope steepness observed through these roads is 23º, which is lower than mean steepness encountered, for instance, through the roads associated with the *HEPP* project (33º) (Fig. 12). This is also the case for two other categories (i.e., *Pre-2010* and *Green Road*). They both cross relatively smooth topography compared to the *HEPP* project. Specifically, the *Green Road* project mainly follows the existing old road path, which passes through ridges (Fig. 3a). Therefore, a predominant part of these roads did not require any hillslope cut in our study area. This explains why the mass

movements triggered in response to the activities of the *HEPP* project gave the largest damage among different construction projects (Fig. 3b).

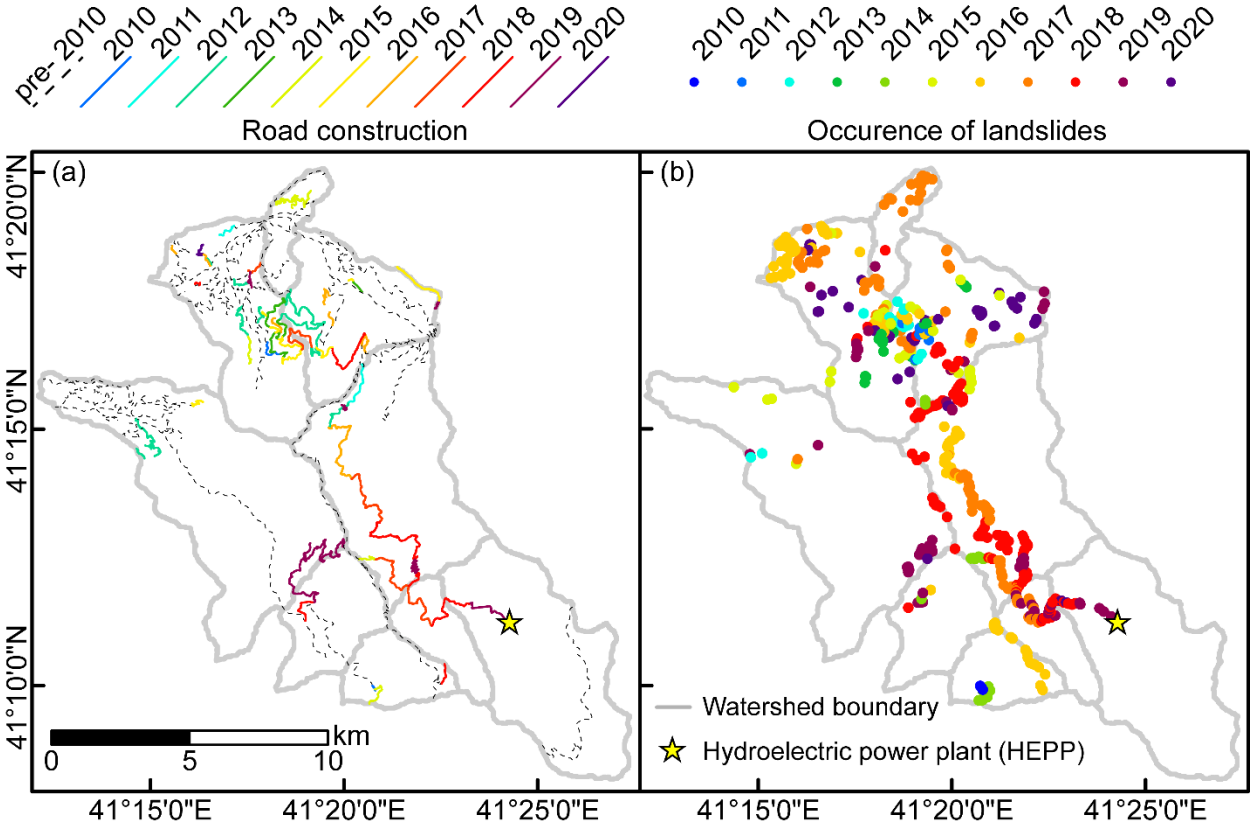

Figure 11. Maps showing the temporal evolution of (a) the roads and (b) the associated landslides.

After 2016, the total length of constructed roads per year increases (see, Fig. 12a). As a result, the number of landslides associated with road construction also significantly increases after 2016. Since then, the contribution of naturally triggered landslides becomes negligible (Fig. 12b).

In 2016, an increase in the landsliding trend could also be linked to strong precipitation (average monthly precipitation was approximately 200 mm/month in 2016). However, in the following years, landslide rates are still higher than pre-2016 levels, although the amount of precipitation is equal or less then the pre-2016 levels (<150 mm/month). These findings indicate that the increase in landslide rate is mostly due to road constructions regardless of extreme rainfall events.

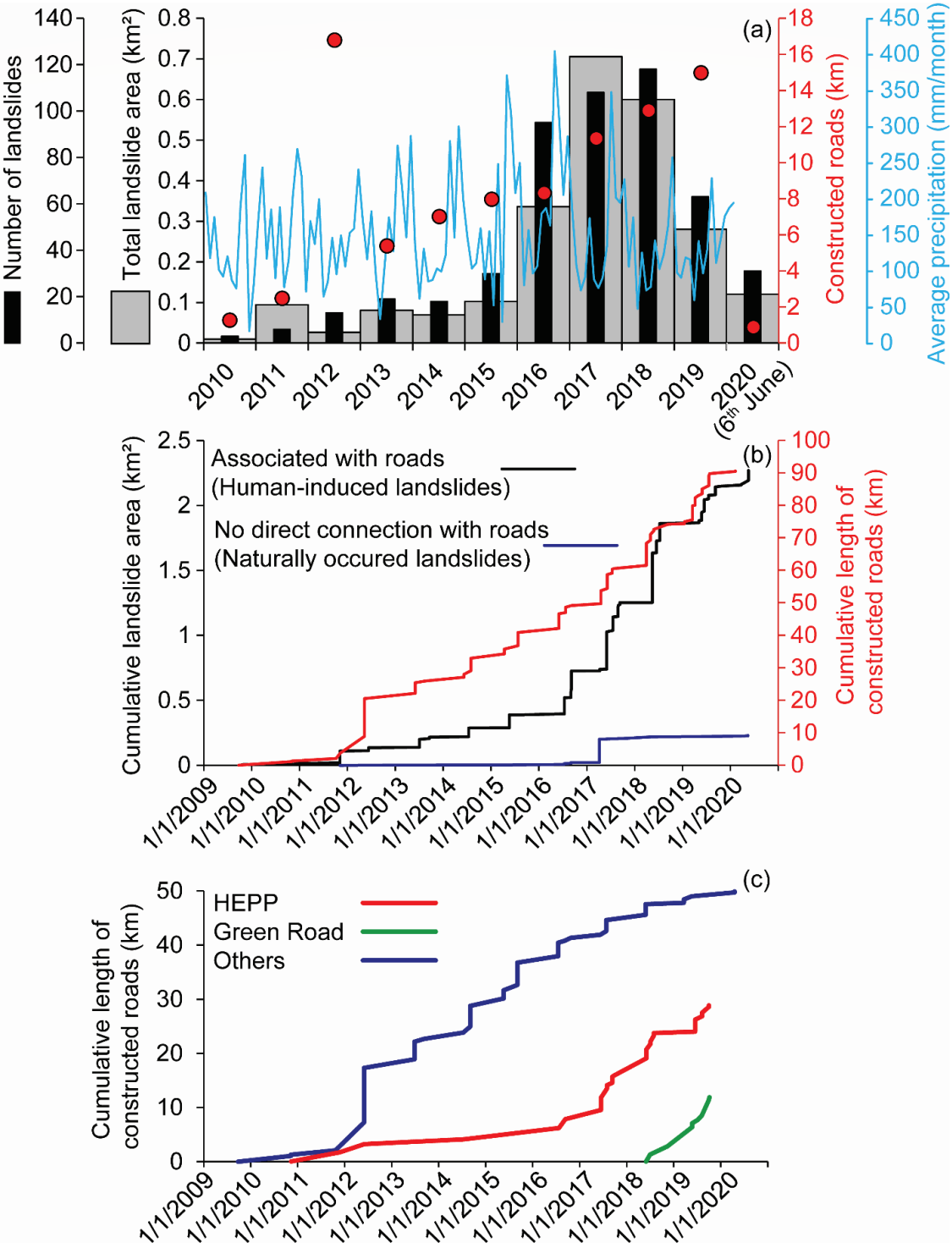

Figure 12. Plots showing the yearly variation in road constructions and landslide occurrences from 2010 to 2020. (a) The number and the total area of landslides against the entire length of

340 constructed roads. (b) The cumulative trend in total landslide size and road length and (c) the
341 roads constructed for different purposes.

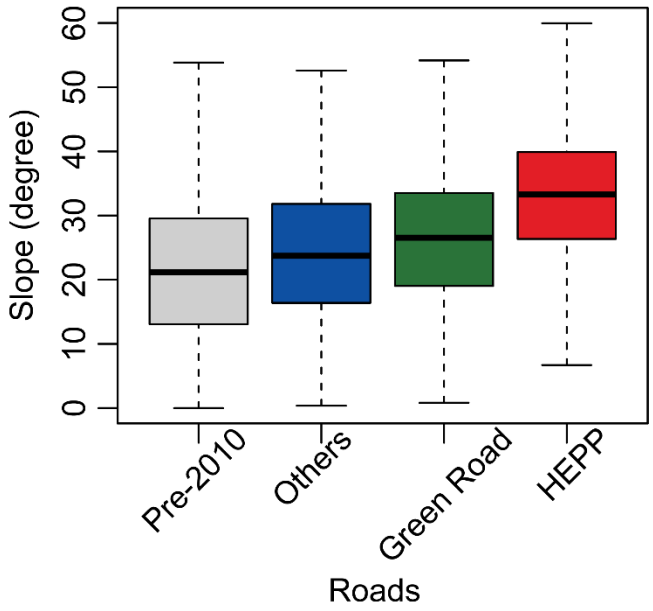

342

343 **Figure 13.** Boxplots showing the range of slope steepness along roads constructed for different
344 purposes.

345 We also examined how the road constructions evolved after 2010 in each catchment and,
346 consequently, how this affected the occurrences of mass movements per hydrological unit.
347 Figure 14 shows the summary of this temporal evolutions. For this analysis, we excluded the
348 naturally occurring landslides. Our findings show that if there is no significant road construction,
349 the number of mass movements is relatively low. For instance, catchments 1, 2, 3 and 4 are
350 adjacent catchments. Among them, catchment 1 is the only hydrological unit where the total
351 length of constructed roads in the last 10 years is less than 5 km. The associated total landslide
352 size in catchment 1 is 0.02 km^2, whereas, in the three other catchments (2,3 and 4), it ranges
353 from 0.24 km^2 to 0.82 km^2. We observed a similar situation in catchments 5, 8 and 9, where we
354 identified a relatively low amount of road constructions (<~5 km) associated with a limited
355 number of landslides (Fig. 14). In catchments 6 and 7, the total length of the road (~10 km) is in
356 between two other sets we mentioned above, but we identified 28 and 9 landslides in these
357 catchments. These roads are mostly associated with the *Green Road* project and thus the limited
358 number of landslides is most likely because of the steepness of the route followed during the
359 construction (Fig. 13).

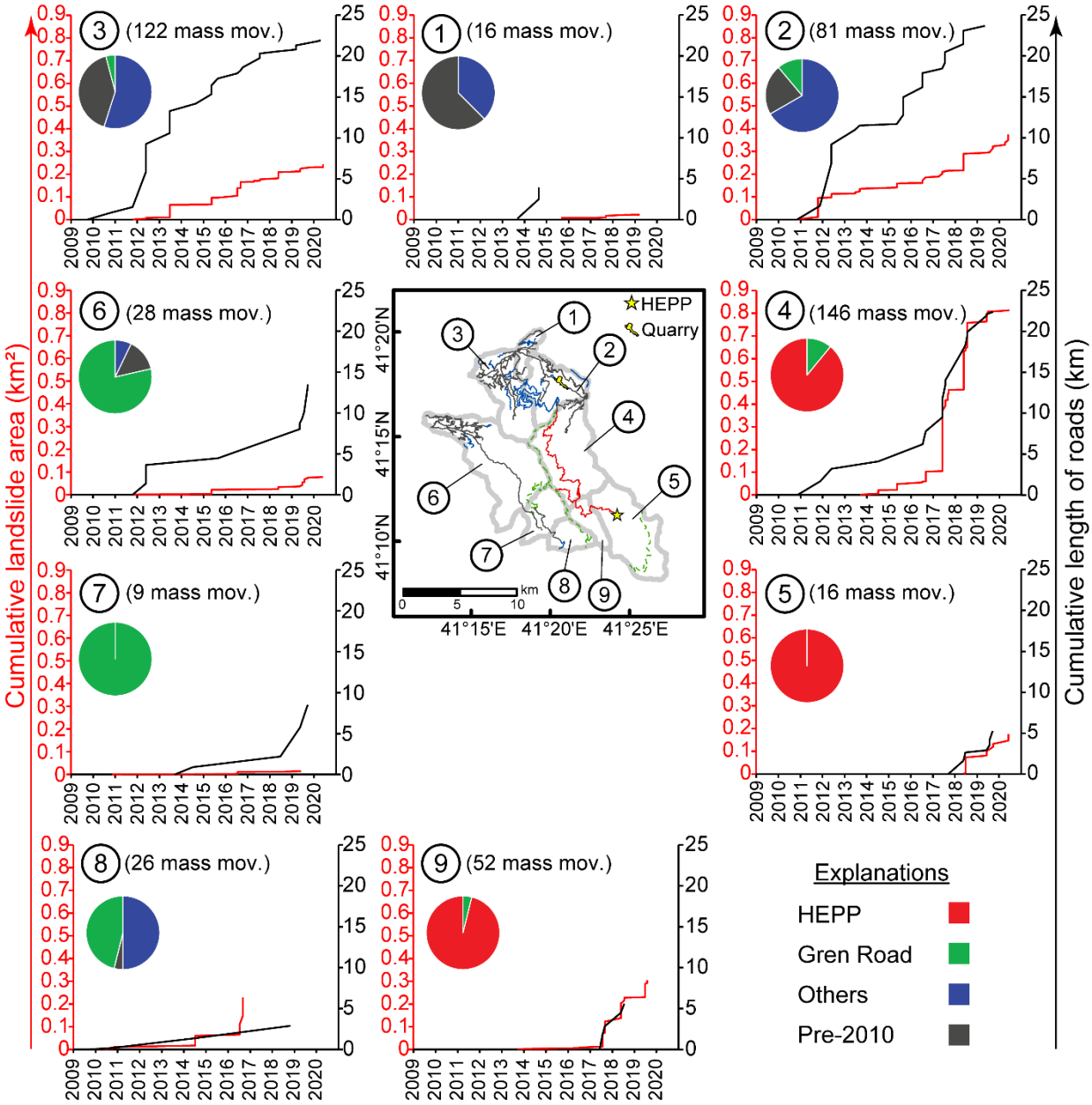

Figure 14. Figure showing the temporal evolution of both roads and landslides within each catchment from 2010 to June 2020. Catchments 2, 3 and 4 appear as hydrological units exposed to the highest road construction and consequently, the largest number of mass movements.

We also compared human-induced landslides with naturally occurred ones in terms of slope steepness and size of landslides. Figure 15 shows that slope steepness of human-induced landslides varies quite broadly compared to naturally occurred landslides. Hillslopes where the

slope steepness ranges from 15º to 50º are associated with a minimum of 20 and a maximum of 100 human-induced landslides. Conversely, the frequency of naturally occurring landslides increases up to 30º (with a minimum of five and a maximum of 15 landslides), and then sharply decreases for steeper slopes. This large difference is undoubtedly induced by road excavations performed on steep slopes, as demonstrated by the much more numerous mass movements that occurred under anthropic disturbance. In fact, the same slope ranges appear to be mostly stable under natural conditions. Also, there is a large difference in average landslide size triggered by road constructions and natural agents. The average size of human-induced landslides is approximately ~20,000 m^2 in the steepest slopes (i.e., 55º-60º), whereas the maximum average size of naturally occurring landslides is ~1000 m^2.

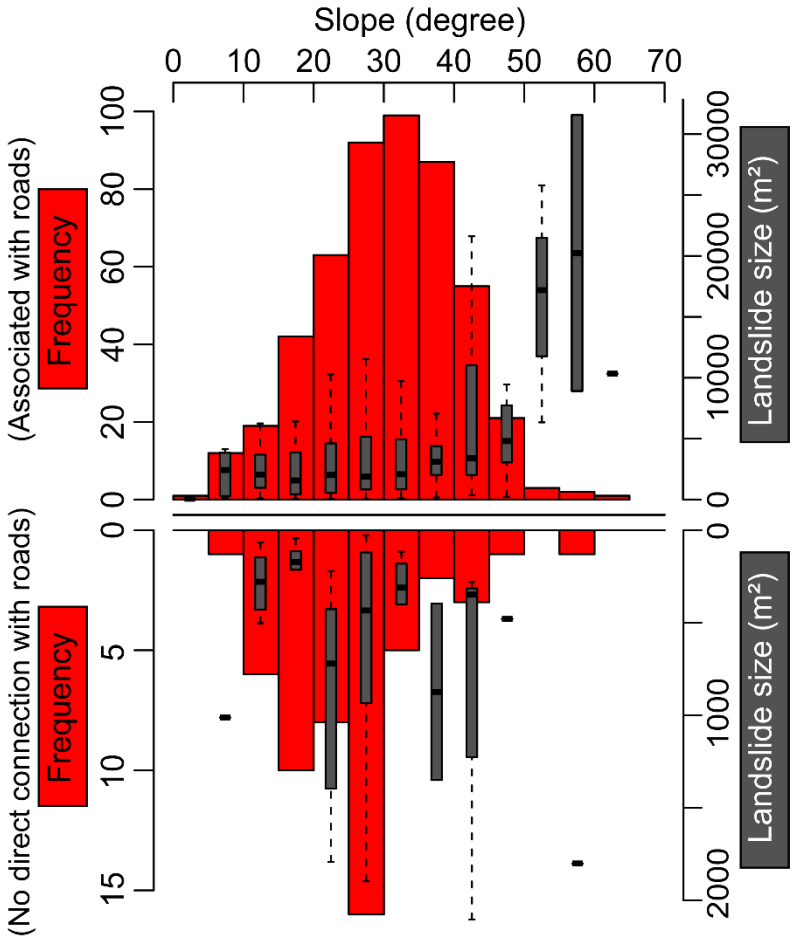

Figure 15. The comparison of human-induced landslides (top panel) with naturally occurred (bottom panel) ones in terms of slope steepness and landslide size characteristics.

5 Discussion

382 In this study, we provide quantitative, thorough systematically mapping mass movement rate
383 after major road constructions in a mountainous region that is exposed to strong precipitation
384 regimes. We specifically chose this region because seismicity does not play an active role here
385 and therefore, capturing the anthropogenic effect on slope stability is more evident than in
386 tectonically active mountainous regions such as Nepal, India or Pakistan. In tectonically active
387 areas, the legacy of previous earthquakes could last for a long period, increasing the landslide
388 susceptibility (R. N. Parker et al., 2015). In particular, after strong earthquakes, the elevated
389 susceptibility is noticeable in the following years (up to nine years) and it decreases over time
390 (e.g., Fan et al., 2018). Consequently, in such environments, it would be challenging to
391 decompose the signal of earthquake legacy from anthropic disturbances. Precipitation could also
392 add another layer of complexity. In fact, the occurrence of a landslide or a population of
393 landslides is always controlled by multiple predisposing and triggering factors (e.g., geotechnical
394 properties, hydrologic conditions, land cover, external loads, etc.,) (e.g., Jaboyedoff et al., 2018).
395 Capturing the relative contribution of each conditional factor requires not only highly detailed
396 temporal landslide inventories -- where we can assess the exact date of occurrence of each
397 landslide -- but also quantitative measurements of the predisposing factors at a given time.
398 Notably, we lack such detailed datasets in this paper, and this is often the case in many landslide
399 susceptibility studies, even when multi-temporal models are built (e.g., Guzzetti et al., 2005).

400 Despite the complexity we faced and the limited temporal information on other controlling
401 factors, we could still investigate whether a relationship exists between slope failures and
402 anthropogenic effect. To address this issue, we made a binary classification distinguishing
403 human-induced and naturally occurring landslides on the basis of satellite images. However, in
404 some cases, this identification was challenging, as well. For instance, the largest landslide we
405 mapped within the region occurred on 7th November 2016, following a strong precipitation event
406 (Ersoy, 2017). This event was a shallow earth-slide flow that affected an area of approximately
407 0.2 km^2 within the Kireçli village (Fig. 16). Satellite images show that the crest of the landslides
408 is precisely aligned with an existing road. Some parts of the road failed as a result of this
409 landslide (Ersoy, 2017). The complexity in the interpretation arose because this landslide could
410 also be linked to natural landscape evolution processes. In fact, the landslide initiated at the ridge
411 of the slope where the susceptibility is generally higher. Thus, the shallow landslide might have
412 been triggered regardless of the possible influence of the road.

In such cases, we labelled landslides as naturally occurring ones since we do not have adequate support to argue that they are human-induced. We did this to implement a conservative approach in our analyses. However, emphasis should still be given to the possible direct or indirect anthropogenic effects. In fact, the road could have a direct implication by increasing the pore water pressure at the crest of the landslide. Also, the external loads associated with traffic might be another likely contributor to the landslide initiation. This event is a very interesting example also because of the existence of an active rock quarry approximately 3 km east. There, to dig into the slope and collect the material explosives are commonly used. Our local contacts informed us that some damages had been observed at houses in villages close to the quarry (i.e., Dikyamaç, Güneşli, Dereüstü villages). Among them, the Dereüstü village is located approximately 2.5 km northwest of the quarry, at a comparable distance to the mudflow location. Therefore, the disturbance exerted by activities related to the quarry might have also played a role in triggering the landslide mentioned above.

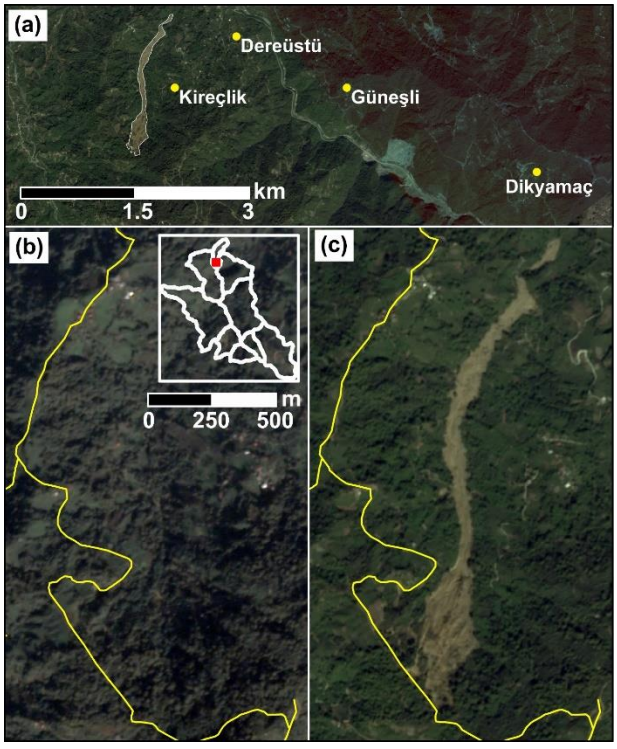

Figure 16. PlanetScope scenes showing the pre- and post- landslide landscape of the largest landslide mapped within the study area (41º 17′ 37″ N and 41º 18′ 27″ E). This landslide occurred on 7th November 2016. The location with respect to our study area is given in the upper right of the panel (b). Yellow lines in the panel (b) and (c) indicate roads.

A similar anthropogenic effect, if not even stronger, could also be valid for landslides triggered along the roads constructed as part of the *HEPP* project, because of the explosives directly used to cut the hillslope. In fact, apart from hillslope cuts, explosives have been used in the last segment of the road approaching the *HEPP* site. In this section, approximately 620 m of the route passes through a tunnel. In such steep terrain, any time a new road is constructed, the damage to the slope is almost inevitable unless extreme precautions are taken. This is also reported in the literature. For instance, Froude and Petley (2018) report that from 2004 to 2016, 30% and 43% of fatal landslides occurred in India and Nepal are associated with road constructions. In these cases, the high landslide rates are not due to the lack of engineering solutions. In fact, landslides triggered in response to road construction projects are a well-known issue for both India and Nepal. The required and appropriate engineering practices necessary to minimize environmental damage have already been documented (e.g., Hearn and Shakya, 2017). The observed landslide hazard associated with road construction is mostly due to neglected engineering solutions (Hearn & Shakya, 2017). Therefore, road construction in mountainous regions should not be envisioned unless the required investment in road design is available (Hearn & Shakya, 2017; Valdiya, 2014). Notably, the site we examined is a good example where road construction has widely damaged the landscape, and it is clear that better precaution or stabilization investments should have been put into practice.

To assess the consequences of human effects on mass movements, we also compared our landslide inventory (i.e., only the landslides associated with road constructions) with nine earthquake-induced landslide-event inventories sharing similar landslide-event magnitude and total landslide area. Figure 17 shows that the human-induced mass movement inventory we mapped is compatible with landslide-events triggered by earthquakes having magnitudes varying from M_w=5.9 to M_w=7.2. This observation is made regardless of climatic and morphologic conditions.

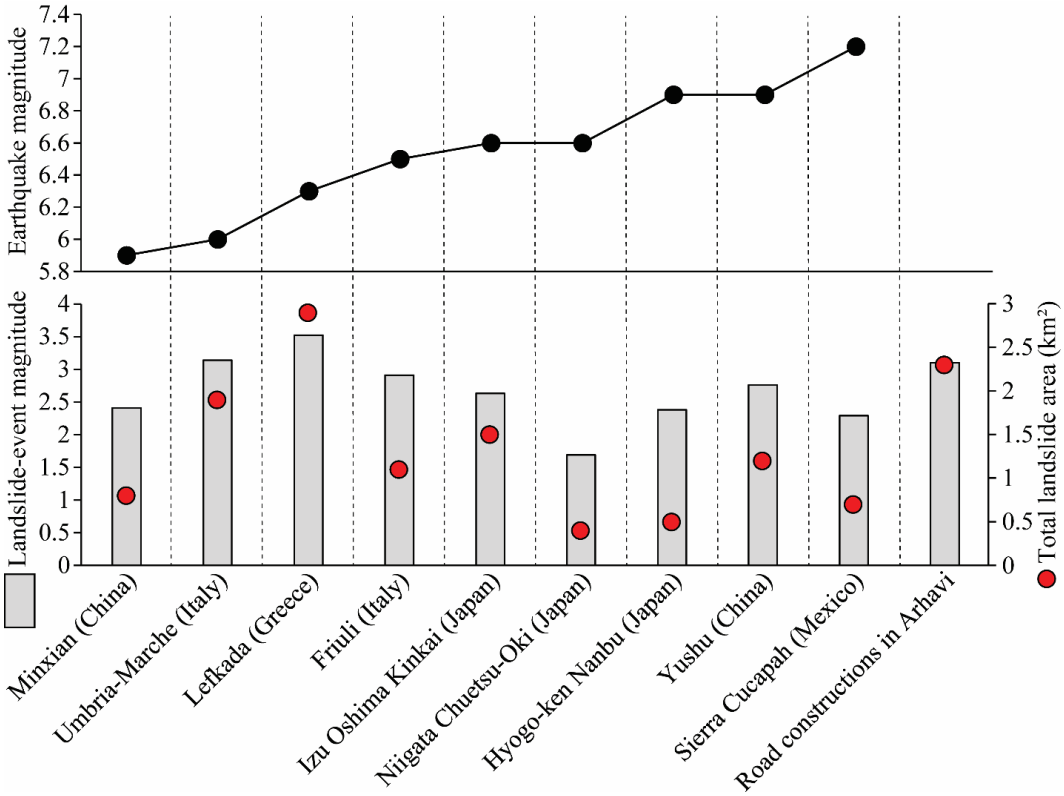

456

457 **Figure 17.** Comparison between our human-induced mass movement inventory and nine
458 earthquake-induced landslide inventories. Landslide-event magnitudes were calculated based on
459 Tanyaş et al. (2018).

460 Among the ten examined cases, the total surface affected by landslides changes significantly
461 from one case to another, with many cases showing a much larger spatial extent compared to our
462 study site. Therefore, for a better comparison, we further investigated the landslide inventory
463 associated with the 2013 Minxian earthquake (M_s=6.6 based on the China Earthquake Network
464 Center and M_w=5.9, according to USGS), where the extent of the region affected by landslides is
465 equivalent to our study area. Specifically, the earthquake occurred between Minxian and
466 Zhangixan (in the Gansu Province, China) on a thrust fault and triggered 2330 co-seismic
467 landslides covering ~200 km^2 (Xu, Xu, Shyu, Zheng, & Min, 2014), which is also compatible
468 with our study area where the examined catchments cover approximately 195 km^2.

469 The cumulated extent of all the landslide polygons associated with the Minxian earthquake is 0.8
470 km^2, whereas the total size of our human-induced landslides is 2.3 km^2. This shows that even the
471 mass movements solely related to the *HEPP* project (total landslide area is 1.3 km^2) can
472 significantly surpass the total co-seismic landslide size induced by the Minxian earthquake.

Before comparing the two inventories in terms of their size statistics, we first analyzed in terms of climatic and morphologic conditions. To collate the climatic information, we used the 20 years (from 2000-06-01 to 2020-03-31) precipitation time series accessed via the IMERG Final Run product, for both sites. Figure 18a shows that both sites have similar precipitation regimes, although the precipitation is relatively higher in our study area. Also, slope and local relief (derived from the SRTM DEM at ~30m) observed in our study area indicate rougher terrain within the landslide-affected area compared to those affected by the Minxian earthquake (Fig. 18b and 18c).

We recognize that the two different sites cannot be thoroughly compared because a much more thorough assessment should be made accounting for detailed geological/geotechnical/hydrological data. However, on the basis of the simplified overview we provide, we can hypothesize that if an earthquake with comparable magnitude to Minxian would occur in our study area, the resultant landslide event should be more significant because our study area is associated with higher precipitation and steeper terrain conditions.

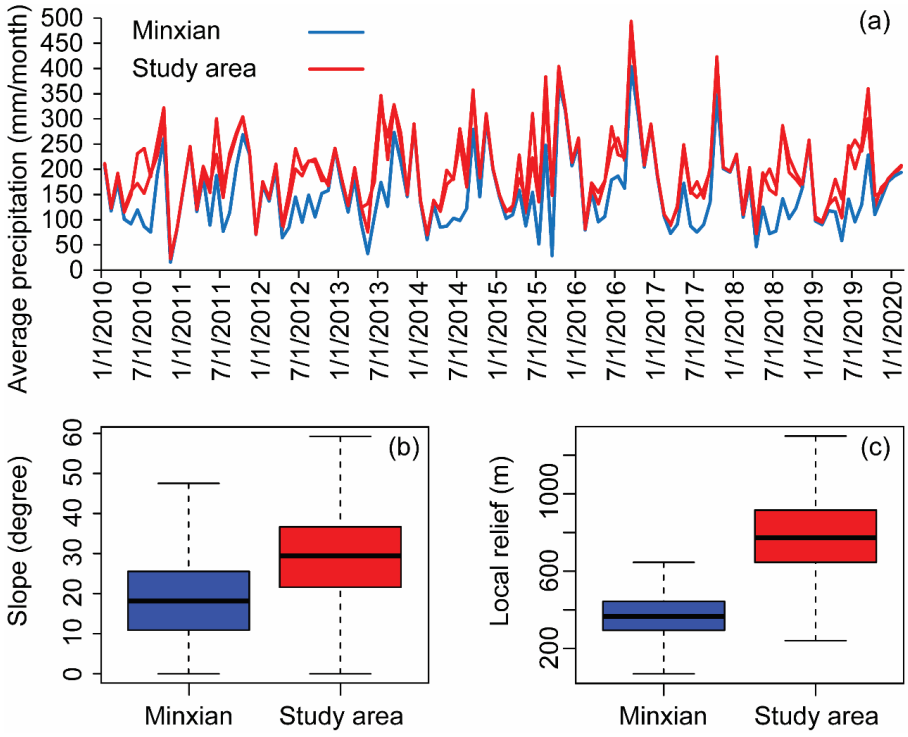

Figure 18. Plots comparing our study area with the landslide affected area of 2013 Minxian earthquake regarding (a) precipitation amounts, (b) slope steepness and (c) local relief.

The comparison between the frequency-density distributions of the human-induced landslides we mapped and those naturally triggered by the 2013 Minxian earthquake shows that larger landslides were triggered in our Turkish site (Fig. 19). The power-law exponents calculated for both our inventory (β=-2.7) and the Minxian inventory (β=-2.3) are close to each other and align well with distributions documented in the literature. In fact, power-law exponents of naturally occurred landslide inventories fall in the range 1.4–3.4, with a central tendency 2.3–2.5 (Stark & Guzzetti, 2009; Tanyaş et al., 2018; Van Den Eeckhaut, Poesen, Govers, Verstraeten, & Demoulin, 2007).

We also calculated the landslide-event magnitudes of our human-induced landslide inventory (mLS=3.1) and the Minxian inventory (mLS=2.4). The difference between the two cases are consistent with our initial assumption that if a similar earthquake occurred in our study area, it would be more disastrous. In fact, based on the empirical relation between earthquake magnitude (M) and landslide-event magnitude scale proposed by Malamud et al. (2004), the earthquake magnitude for an equivalent earthquake-induced landslide inventory would be 6.8. This shows how destructive the anthropogenic effect on geomorphological processes could be compared to natural processes. The destruction produced by the road constructions conducted in the last 10 years is compatible with the possible effect of a theoretical earthquake with a magnitude greater than 6.0.

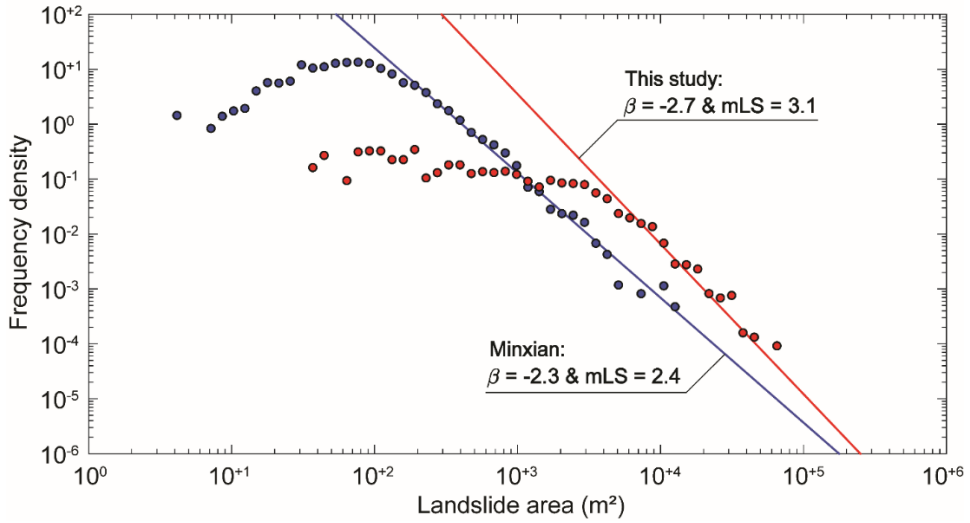

Figure 19. Frequency-density curves plotted for the landslides associated with roads in our study area (red) and landslide triggered by the 2013 Minxian earthquake (blue). Power-law exponents

(β) were calculated based on the method proposed by Clauset et al. (2009), whereas power-law fits and landslide-event magnitudes were identified based on Tanyaş et al. (2018).

6 Conclusions

In this study, we report a distinct correlation of mass movements and major road constructions that explicitly shows human impact on mountainous environments which are under anthropogenic disturbance recently. Our results further suggest that slope instabilities increased drastically after major service road constructions for hydroelectric power plants and as well as other road extension works. Despite the high precipitation amounts in the region, naturally occurring landslides represent a minor percentage both in number and landslide-size-characteristics when compared to the equivalent human-induced mass movements. Regardless of the natural hillslope processes at play, the poor implementation of engineering practices able to ensure stable slope conditions in co- and post- construction phases not only resulted in dangerous widespread landslides but also caused a substantial change in the sediment transport along with the river network. We could not access enough information on the potential effects of this to quantify increases in sediment loads. However, in the long term, the coarse nature of the material removed from the slopes could also clog narrow river passages, potentially damming small sections of the river network. This could further induce a chain of disastrous events, which could affect not only people living nearby but also the rich biodiversity of the region that needs to be protected. This actually means that all endemic-rare plant and animal species exist in Kamilet Valley are in danger now because of the poor engineering practice. Our results emphasize the need to consider erosion and post changes in hillslope processes and sediment flux that further lead to additional threats to the local community and biodiversity in response to poor engineering practices any other anthropogenic disturbances.

We also stress that the impact of road construction can disturb the natural slope equilibrium to an extent comparable with moderate (larger than 6 M_w) earthquakes. Such an observation implies that human activities can have a large, if not even dominant, impact on landscape evolution and the natural regime of surface processes. This is part of the definition of Anthropocene, an age where our society shapes nature for our purposes, frequently at the risk of damaging ourselves.

Acknowledgments

We are very grateful to Hasan Sıtkı Özkazanç, an environmental activist from Arhavi Doğa Koruma Platformu, for providing us valuable information regarding the road constructions and their consequences in the site. Co-seismic landslide inventories we examined are available from Schmitt et al. (2017) (https://www.sciencebase.gov/catalog/item/583f4114e4b04fc80e3c4a1a). The inventories we mapped for this study are shared through NASA Landslide Viewer (https://landslides.nasa.gov).

References

Akbulut, S., & Kurdoglu, O. (2015). Türkiye'de acil ve öncelikle korunmasi gereken bir alan: Kamilet ve Durguna Vadileri (Arhavi) ve koruma gerekçeleri. *Kastamonu Üniversitesi Orman Fakültesi Dergisi*, *15*(2), 279-296 (in Turkish).

Alan, I., Balci, V., Keskin, H., Altun, I., Boke, N., Demirbag, H., … Hanilci, N. (2019). Tectonostratigraphic characteristics of the area between Çayeli (Rize) and Ispir (Erzurum). *Maden Tetkik ve Arama Dergisi*, *158*(158), 1–29.

Atta-ur-Rahman, Khan, A. N., Collins, A. E., & Qazi, F. (2011). Causes and extent of environmental impacts of landslide hazard in the Himalayan region: a case study of Murree, Pakistan. *Natural Hazards*, *57*(2), 413–434. https://doi.org/10.1007/s11069-010-9621-7

Barnard, P. L., Owen, L. A., Sharma, M. C., & Finkel, R. C. (2001). Natural and human-induced landsliding in the Garhwal Himalaya of northern India. *Geomorphology*, *40*(1), 21–35. https://doi.org/https://doi.org/10.1016/S0169-555X(01)00035-6

Brown, A. G., Tooth, S., Bullard, J. E., Thomas, D. S. G., Chiverrell, R. C., Plater, A. J., … Aalto, R. (2017). The geomorphology of the Anthropocene: emergence, status and implications. *Earth Surface Processes and Landforms*, *42*(1), 71–90. https://doi.org/10.1002/esp.3943

Brown, A. G., Tooth, S., Chiverrell, R. C., Rose, J., Thomas, D. S. G., Wainwright, J., … Downs, P. (2013). The Anthropocene: is there a geomorphological case? *Earth Surface Processes and Landforms*, *38*(4), 431–434. https://doi.org/10.1002/esp.3368

Chang, J., & Slaymaker, O. (2002). Frequency and spatial distribution of landslides in a mountainous drainage basin: Western Foothills, Taiwan. *CATENA*, *46*(4), 285–307.

https://doi.org/https://doi.org/10.1016/S0341-8162(01)00157-6

Chen, Y.-J., & Chang, K.-C. (2011). A spatial–temporal analysis of impacts from human development on the Shih-men Reservoir watershed, Taiwan. *International Journal of Remote Sensing*, *32*(24), 9473–9496. https://doi.org/10.1080/01431161.2011.562253

Clauset, A., Shalizi, C. R., & Newman, M. E. J. (2009). Power-law distributions in empirical data. *SIAM Review*, *51*(4), 661–703. https://doi.org/10.1137/070710111

Coker, R. J., & Fahey, B. D. (1993). Road-related mass movement in weathered granite, Golden Downs and Motueka Forests, New Zealand: a note. *Journal of Hydrology (New Zealand)*, *31*(1), 65–69. Retrieved from http://www.jstor.org/stable/43944699

Dadson, S. J., Hovius, N., Chen, H., Dade, W. B., Lin, J.-C., Hsu, M.-L., … Stark, C. P. (2004). Earthquake-triggered increase in sediment delivery from an active mountain belt. *Geology*, *32*(8), 733–736. https://doi.org/10.1130/G20639.1

DOKAP. (2014). *Doğu Karadeniz Projesi (DOKAP) Eylem Planı (2014-2018)*.

Ersoy, S. (2017). *2016 Yılı Doğa Kaynaklı Afetler Yıllığı "Dünya ve Türkiye."* Jeoloji Mühendisleri Odası Yayınları No: 129, Ankara (in Turkish).

Fan, X., Domènech, G., Scaringi, G., Huang, R., Xu, Q., Hales, T. C., … Francis, O. (2018). Spatio-temporal evolution of mass wasting after the 2008 Mw 7.9 Wenchuan earthquake revealed by a detailed multi-temporal inventory. *Landslides*, *15*(12), 2325–2341. https://doi.org/10.1007/s10346-018-1054-5

Fransen, P. J. B., Phillips, C. J., & Fahey, B. D. (2001). Forest road erosion in New Zealand: overview. *Earth Surface Processes and Landforms*, *26*(2), 165–174. https://doi.org/10.1002/1096-9837(200102)26:2<165::AID-ESP170>3.0.CO;2-#

Froude, M. J., & Petley, D. N. (2018). Global fatal landslide occurrence from 2004 to 2016. *Natural Hazards and Earth System Sciences*, *18*(8), 2161–2181. https://doi.org/10.5194/nhess-18-2161-2018

Guzzetti, F., Malamud, B. D., Turcotte, D. L., & Reichenbach, P. (2002). Power-law correlations of landslide areas in central Italy. *Earth and Planetary Science Letters*, *195*(3–4), 169–183.

https://doi.org/10.1016/S0012-821X(01)00589-1

Haigh, M. J., Rawat, J. S., & Bartarya, S. K. (1989). Environmental Indicators of Landslide Activity along the Kilbury Road, Nainital, Kumaun Lesser Himalaya. *Mountain Research and Development*, *9*(1), 25–33. https://doi.org/10.2307/3673462

Hearn, G. J., & Shakya, N. M. (2017). Engineering challenges for sustainable road access in the Himalayas. *Quarterly Journal of Engineering Geology and Hydrogeology*, *50*(1), 69–80. https://doi.org/10.1144/qjegh2016-109

Holcombe, E. A., Beesley, M. E. W., Vardanega, P. J., & Sorbie, R. (2016). Urbanisation and landslides: hazard drivers and better practices. *Proceedings of the Institution of Civil Engineers - Civil Engineering*, *169*(3), 137–144. https://doi.org/10.1680/jcien.15.00044

Huffman, G., Stocker, E. F., T, B. D., Nelkin, E. J., & Tan, J. (2019). GPM IMERG Final Precipitation L3 1 day 0.1 degree x 0.1 degree V06. *Edited by Andrey Savtchenko, Greenbelt, MD, Goddard Earth Sciences Data and Information Services Center (GES DISC)*.

Jaboyedoff, M., Michoud, C., Derron, M. H., Voumard, J., Leibundgut, G., Sudmeier-Rieux, K., … Leroi, E. (2018). Human-induced landslides: Toward the analysis of anthropogenic changes of the slope environment. *Landslides and Engineered Slopes. Experience, Theory and Practice; CRC Press: Boca Raton, FL, USA*, 217–232.

Jones, J., Boulton, S., Bennett, G., Whitworth, M., & Stokes, M. (2020). Himalaya mass-wasting: impacts of the monsoon, extreme tectonic and climatic forcing, and road construction. *EGU General Assembly 2020*. https://doi.org/https://doi.org/10.5194/egusphere-egu2020-8702

Khan, S. F., Kamp, U., & Owen, L. A. (2013). Documenting five years of landsliding after the 2005 Kashmir earthquake, using repeat photography. *Geomorphology*, *197*, 45–55. https://doi.org/10.1016/j.geomorph.2013.04.033

Khattak, G. A., Owen, L. A., Kamp, U., & Harp, E. L. (2010). Evolution of earthquake-triggered landslides in the Kashmir Himalaya, northern Pakistan. *Geomorphology*, *115*(1–2), 102–108. https://doi.org/10.1016/j.geomorph.2009.09.035

623 Larsen, M. C., & Parks, J. E. (1997). How wide is a road? The association of roads and mass-
624 wasting in a forested montane environment. *Earth Surface Processes and Landforms: The*
625 *Journal of the British Geomorphological Group*, *22*(9), 835–848.

626 Lewis, S. L., & Maslin, M. A. (2015). Defining the Anthropocene. *Nature*, *519*, 171+.

627 Malamud, B. D., Turcotte, D. L., Guzzetti, F., & Reichenbach, P. (2004). Landslide inventories
628 and their statistical properties. *Earth Surface Processes and Landforms*, *29*(6), 687–711.
629 https://doi.org/10.1002/esp.1064

630 McAdoo, B. G., Quak, M., Gnyawali, K. R., Adhikari, B. R., Devkota, S., Rajbhandari, P. L., &
631 Sudmeier-Rieux, K. (2018). Roads and landslides in Nepal: how development affects
632 environmental risk. *Natural Hazards and Earth System Sciences*, *18*(12), 3203–3210.
633 https://doi.org/10.5194/nhess-18-3203-2018

634 Morin, G. P., Lavé, J., France-Lanord, C., Rigaudier, T., Gajurel, A. P., & Sinha, R. (2018).
635 Annual Sediment Transport Dynamics in the Narayani Basin, Central Nepal: Assessing the
636 Impacts of Erosion Processes in the Annual Sediment Budget. *Journal of Geophysical*
637 *Research: Earth Surface*, *123*(10), 2341–2376. https://doi.org/10.1029/2017JF004460

638 MTA. (2002). 1:500 000–scale map of Turkey. *General Directorate of Mineral Research and*
639 *Exploration (MTA), Ankara, Turkey*.

640 NASA JPL. (2013). NASA Shuttle Radar Topography Mission United States 1 Arc Second.
641 NASA EOSDIS Land Processes DAAC, USGS Earth Resources Observation and Science
642 (EROS) Center, Sioux Falls, South Dakota https://lpdaac.usgs.gov, Accessed date: 1
643 December 2019. Retrieved from
644 https://doi.org/10.5067/MEaSUREs/SRTM/SRTMUS1.003

645 Nefeslioglu, H. A., Gokceoglu, C., Sonmez, H., & Gorum, T. (2011). Medium-scale hazard
646 mapping for shallow landslide initiation: the Buyukkoy catchment area (Cayeli, Rize,
647 Turkey). *Landslides*, *8*(4), 459–483. https://doi.org/10.1007/s10346-011-0267-7

648 Owen, L. A., Kamp, U., Khattak, G. A., Harp, E. L., Keefer, D. K., & Bauer, M. A. (2008).
649 Landslides triggered by the 8 October 2005 Kashmir earthquake. *Geomorphology*, *94*(1–2),
650 1–9. https://doi.org/10.1016/j.geomorph.2007.04.007

Parker, R. N., Hancox, G. T., Petley, D. N., Massey, C. I., Densmore, A. L., & Rosser, N. J. (2015). Spatial distributions of earthquake-induced landslides and hillslope preconditioning in the northwest South Island, New Zealand. *Earth Surface Dynamics*, *3*(4), 501–525. https://doi.org/10.5194/esurf-3-501-2015

Parker, Robert N., Densmore, A. L., Rosser, N. J., De Michele, M., Li, Y., Huang, R., … Petley, D. N. (2011). Mass wasting triggered by the 2008 Wenchuan earthquake is greater than orogenic growth. *Nature Geoscience*, *4*(7), 449–452. https://doi.org/10.1038/ngeo1154

Petley, D. (2012). Global patterns of loss of life from landslides. *Geology*, *40*(10), 927–930. https://doi.org/10.1130/G33217.1

Petley, D. N., Hearn, G. J., Hart, A., Rosser, N. J., Dunning, S. A., Oven, K., & Mitchell, W. A. (2007). Trends in landslide occurrence in Nepal. *Natural Hazards*, *43*(1), 23–44. https://doi.org/10.1007/s11069-006-9100-3

Planet Team. (2017). Planet Application Program Interface: In Space for Life on Earth. San Francisco, CA. https://api.planet.com.

Poesen, J. (2018). Soil erosion in the Anthropocene: Research needs. *Earth Surface Processes and Landforms*, *43*(1), 64–84. https://doi.org/10.1002/esp.4250

Raja, N. B., Çiçek, I., Türkoğlu, N., Aydin, O., & Kawasaki, A. (2017). Landslide susceptibility mapping of the Sera River Basin using logistic regression model. *Natural Hazards*, *85*(3), 1323–1346. https://doi.org/10.1007/s11069-016-2591-7

Reis, S., Nişanci, R., & Yomralioğlu, T. (2009). Designing and Developing a Province-Based Spatial Database for the Analysis of Potential Environmental Issues in Trabzon, Turkey. *Environmental Engineering Science*, *26*(1), 123–130. https://doi.org/10.1089/ees.2007.0158

Schmitt, R. G., Tanyas, H., Nowicki Jessee, M. A., Zhu, J., Biegel, K. M., Allstadt, K. E., … Knudsen, K. L. (2017). An open repository of earthquake-triggered ground-failure inventories. In *Data Series*. https://doi.org/10.3133/ds1064

Şekercioğlu, Ç. H., Anderson, S., Akçay, E., & Bilgin, R. (2011). Turkey's rich natural heritage under assault. *Science*, *334*(6063), 1637–1639.

678 Şekercioğlu, Ç. H., Anderson, S., Akçay, E., Bilgin, R., Can, Ö. E., Semiz, G., … Nüzhet Dalfes,
679 H. (2011). Turkey's globally important biodiversity in crisis. *Biological Conservation*,
680 *144*(12), 2752–2769. https://doi.org/https://doi.org/10.1016/j.biocon.2011.06.025

681 Stark, C. P., & Guzzetti, F. (2009). Landslide rupture and the probability distribution of
682 mobilized debris volumes. *Journal of Geophysical Research: Earth Surface*, *114*(2), 1–16.
683 https://doi.org/10.1029/2008JF001008

684 Steffen, W., Broadgate, W., Deutsch, L., Gaffney, O., & Ludwig, C. (2015). The trajectory of the
685 Anthropocene: The Great Acceleration. *The Anthropocene Review*, *2*(1), 81–98.
686 https://doi.org/10.1177/2053019614564785

687 Steffen, W., Grinevald, J., Crutzen, P., & McNeill, John. (2011). The Anthropocene: conceptual
688 and historical perspectives. *Philosophical Transactions of the Royal Society A:*
689 *Mathematical, Physical and Engineering Sciences*, *369*(1938), 842–867.
690 https://doi.org/10.1098/rsta.2010.0327

691 Tang, C., Zhu, J., Qi, X., & Ding, J. (2011). Landslides induced by the Wenchuan earthquake
692 and the subsequent strong rainfall event: A case study in the Beichuan area of China.
693 *Engineering Geology*, *122*(1), 22–33.
694 https://doi.org/https://doi.org/10.1016/j.enggeo.2011.03.013

695 Tanyaş, H., Allstadt, K. E., & van Westen, C. J. (2018). An updated method for estimating
696 landslide-event magnitude. *Earth Surface Processes and Landforms*, *43*(9).
697 https://doi.org/10.1002/esp.4359

698 Tanyaş, H., van Westen, C. J., Allstadt, K. E., Anna Nowicki Jessee, M., Görüm, T., Jibson, R.
699 W., … Hovius, N. (2017). Presentation and Analysis of a Worldwide Database of
700 Earthquake-Induced Landslide Inventories. *Journal of Geophysical Research: Earth*
701 *Surface*, *122*(10). https://doi.org/10.1002/2017JF004236

702 Tanyaş, H., van Westen, C. J., Allstadt, K. E., & Jibson, R. W. (2019). Factors controlling
703 landslide frequency–area distributions. *Earth Surface Processes and Landforms*, *44*(4).
704 https://doi.org/10.1002/esp.4543

705 U.S. Geological Survey. (2017). Search Earthquake Catalog. Retrieved March 2, 2020, from

https://earthquake.usgs.gov/earthquakes/search/

Valdiya, K. S. (2014). Damming rivers in the tectonically resurgent Uttarakhand Himalaya. *Current Science*, *106*(12), 1658–1668. Retrieved from http://www.jstor.org/stable/24102998

Van Den Eeckhaut, M., Poesen, J., Govers, G., Verstraeten, G., & Demoulin, A. (2007). Characteristics of the size distribution of recent and historical landslides in a populated hilly region. *Earth and Planetary Science Letters*, *256*(3–4), 588–603. https://doi.org/10.1016/j.epsl.2007.01.040

Vuillez, C., Tonini, M., Sudmeier-Rieux, K., Devkota, S., Derron, M.-H., & Jaboyedoff, M. (2018). Land use changes, landslides and roads in the Phewa Watershed, Western Nepal from 1979 to 2016. *Applied Geography*, *94*, 30–40. https://doi.org/https://doi.org/10.1016/j.apgeog.2018.03.003

Waters, C. N., Zalasiewicz, J., Summerhayes, C., Barnosky, A. D., Poirier, C., Gałuszka, A., … Wolfe, A. P. (2016). The Anthropocene is functionally and stratigraphically distinct from the Holocene. *Science*, *351*(6269), aad2622. https://doi.org/10.1126/science.aad2622

WWF. (2020). Kamilet Havzası Bir Doğa Müzesi Olarak Saklanmalı. Retrieved from https://www.wwf.org.tr/yayinlarimiz/basin_bultenleri/?10060/Kamilet-Havzasi-Bir-Doga-Muzesi-Olarak-Saklanmali

Xu, C., Xu, X., Shyu, J. B. H., Zheng, W., & Min, W. (2014). Landslides triggered by the 22 July 2013 Minxian-Zhangxian, China, Mw 5.9 earthquake: Inventory compiling and spatial distribution analysis. *Journal of Asian Earth Sciences*, *92*(July 2013), 125–142. https://doi.org/10.1016/j.jseaes.2014.06.014

Yuksel, E., & Eminagaoglu, O. (2017). Flora Of The Kamilet Valley (Arhavi, Artvin, Turkey). *International Journal of Ecosystems and Ecology Science-IJEES*, *7*(4), 905–914.

733